CONTROL-THEORY AND ADVANCED TECHNOLOGY
Vol. 10, No. 4, Part 4, pp. 1591-1618, November, 1995

C93131R

Contributed Paper

ENERGY FLOW CONTROL OF INTERCONNECTED STRUCTURES: II. STRUCTURAL SUBSYSTEMS*

Y. KISHIMOTO,[1] D. S. BERNSTEIN[2] AND S. R. HALL[3]

Abstract. The dissipative energy flow control technique for interconnected modal subsystems developed in a companion paper (Kishimoto et al., 1995 b) is now applied to structural subsystems. In this paper, two energy flow models for interconnected structures are derived, namely, the modal subsystem model, which views each mode as a subsystem, and the structural subsystem model, which views each substructure as a subsystem. These energy flow models provide alternative foundations for an energy flow control technique. Active feedback controllers based on both of these energy flow models are shown to reduce the vibration of a specified substructure.

Key Words—Energy flow, control of flexible structures.

1. Introduction

In a companion paper (Kishimoto et al., 1995 b), active energy flow control techniques were considered for interconnected modal subsystems. These techniques are now applied to interconnected structural subsystems. For this purpose, we extend results given in Kishimoto and Bernstein (1995 a; b) and derive two energy flow models for structures interconnected either conservatively or dissipatively. In the modal subsystem model considered in Kishimoto et al. (1995 b), each mode is viewed as a subsystem, while in the structural subsystem model each substructure is treated as a subsystem. For the modal subsystem model we can directly apply the control techniques considered in Kishimoto et al. (1995 b). The structural subsystem model, however, requires special care. In particular, a dissipation filter and a disturbance filter are required since now the real part of the substructure impedance and the disturbance spectral density are frequency-dependent.

Two distinct energy flow control techniques developed in Kishimoto et al. (1995 b) are applied to the modal subsystem model and the structural subsystem model. Specifically, the controller is designed either as an additional subsystem or as a dissipative coupling to minimize energy flow entering a specified substructure. The goal in Kishimoto et al. (1995 b) was to maximize the energy flow

* Received by the editors November 1, 1993 and in revised form November 14, 1994.
This research was supported in part by the Air Force Office of Scientific Research under Grant F49620-92-J-0127 and the NASA SERC Grant NAGW-1335.

[1] Kougi-Tai Hijitsu-Gun, Gifu Air Base, Mubanchi Naka Kanyuchi, Gifu 504, Japan.
[2] Department of Aerospace Engineering, The University of Michigan, Ann Arbor, MI 48109-2118, U.S.A.
[3] Department of Aeronautics and Astronautics, Massachusetts Institute of Technology, Cambridge, MA 02139, U.S.A.

from a specified subsystem in the modal subsystem model and thus reduce the vibration of this substructure.

In previous works (Miller et al., 1990; MacMartin and Hall, 1991), H_2 and H_∞ control techniques were used to regulate energy flow in a certain frequency band. In this paper, as in Kishimoto et al. (1995 b), controllers are designed according to a specialized LQG positive real control approach that yields positive real controllers. Thus, the resulting controller minimizes an H_2 performance index and guarantees asymptotic stability of the closed-loop system in spite of modeling uncertainty.

Illustrative examples involving Bernoulli-Euler beams show that the resulting controllers successfully minimize energy flow into a specified structure and thus reduce the vibration of the structure.

Notation.

R_{xy}: cross correlation function matrix of x and y
S_{xx}: power spectral density matrix of x
S_{xy}: cross spectral density matrix of x and y
j: $\sqrt{-1}$
e_i: ith column of I
$a_{(i)}$: ith element of column vector a
$A_{(k,l)}$: (k, l)-element of A
$A_{[k,l]}$: 2×2 block matrix of (k, l) portion of A
A_{ijkl}: $A_{(n_{ij}, n_{kl})}$
$A_{[ijkl]}$: $A_{[n_{ij}, n_{kl}]}$
$\mathrm{Re}[A]$, $\mathrm{Im}[A]$: real, imaginary part of A
$\mathrm{diag}(a_1, \cdots, a_r)$: diagonal matrix whose ith diagonal element is a_i
A^T, A^*: transpose, complex conjugate transpose of A
$\mathrm{tr}[A]$: trace of A
$A > (\geq) 0$: symmetric positive (nonnegative) definite matrix
$G(s) \sim \left[\begin{array}{c|c} A & B \\ \hline C & D \end{array}\right]$: state space realization of the transfer function

$$G(s) = C(sI - A)^{-1}B + D$$

a_{ij}, b_{ij}: modal coefficients
(A_L, B_L, C_L, D_L): state space model for coupling $L(s)$
(A_m, B_m, C_m, D_m): state space model for modal subsystem model
(A_s, B_s, C_s, D_s): state space model for structural subsystem model
(A_R, B_R, C_R, D_R): state space model for dissipation filter $R_d(s)$
(A_w, B_w, C_w, D_w): state space model for disturbance filter $T(s)$
$(\tilde{A}_m, \tilde{D}_m)$: augmented matrices for modal subsystem model
$(\tilde{A}_s, \tilde{D}_s)$: augmented matrices for structural subsystem model
$(\tilde{A}_d, \tilde{D}_d)$: augmented matrices for dissipation of structural subsystem model
D_m: disturbance matrix for modal subsystem model
$E_i I_{Ai}$: bending stiffness of ith beam
$f_i(t)$: coupling force interaction
$g_i(t)$: coupling moment interaction
$h_i(\xi, \xi_{ci}, t)$: coupling effect
I: identity matrix

k_{ij}: wave number
K_{ij}: coupling stiffness between i, jth subsystems
$L(s)$: linear time-invariant coupling matrix
$L_m(s)$: linear time-invariant coupling matrix for modal subsystem model
L_i: length of ith beam
$\mathscr{L}_i$: stiffness operator
n_{ij}: counter for modal subsystem
P_i^c (P_{ij}^c): steady-state average coupling energy flow of $i(n_{ij})$th subsystem
P_i^d (P_{ij}^d): steady-state average energy dissipation rate of $i(n_{ij})$th subsystem
P_i^e (P_{ij}^e): steady-state average external power of $i(n_{ij})$th subsystem
$\tilde{Q}_m$: steady-state covariance for modal subsystem model
$\tilde{Q}_s$: steady-state covariance for structural subsystem model
$q_{ij}(t)$: modal coordinate
$R_d(s)$: dissipation filter for structural subsystem model
$T(s)$: disturbance filter for structural subsystem model
$S_{w_m w_m}$: intensity matrix of entering disturbance for modal subsystem model
$\tilde{w}_i(t)$: normalized white noise disturbance with unit intensity
$w_i(t), (w_{ij}(t))$: disturbance entering substructure (mode)
$Z_m(s)$: subsystem impedance matrix for modal subsystem model
$Z_s(s)$: subsystem impedance matrix for structural subsystem model
$z_i(s), z_{ij}(s)$: subsystem (impedance transfer function)
ζ_i: structural damping coefficient
$\chi(\xi, t)$: modal decomposition
ξ: structural coordinate
ξ_{ci}: coupling position of ith structure
$\hat{\xi}_i$: disturbance entering position of ith structure
$\rho_{(i)}$: mass density (of ith structure)
$\psi_{ij}(\xi)$: eigenfunction of jth mode of ith structure
ω_{ij}: natural frequency of jth mode of ith structure

2. Structural Model

We consider r one- or two-dimensional structures under vibration by means of pointwise external disturbance forces. Each pair of structures is assumed to be mutually interconnected by means of conservative or dissipative couplings. For convenience, we make the simplifying assumption that all couplings to a given structure are connected to a single point on that structure. The case of structures interconnected at multiple points is more complicated and is outside the scope of this paper.

The partial differential equation for the response of the ith structure is given by

$$\rho_i(\xi)\frac{\partial^2 \chi_i(\xi, t)}{\partial t^2} + \mathscr{L}_i \chi_i(\xi, t) = \tilde{w}_i(t)\delta(\xi - \hat{\xi}_i) - h_i(\xi, \xi_{ci}, t), \qquad (1)$$

where $\xi \in \Omega_i$ denotes the spatial coordinate defined on the region of space Ω_i for the ith structure. Furthermore, $\rho_i(\xi)$ is the mass density, $\mathscr{L}_i$ is the self-adjoint stiffness operator for the ith structure, and $\tilde{w}_i(t)$ is the external disturbance force acting on the ith structure at the point ξ_i. We assume that $\tilde{w}_i(t)$, $i = 1, \cdots, r$, are mutually uncorrelated white noise disturbances with unit intensity. Additionally, the coupling effect $h_i(\xi, \xi_{ci}, t)$ at the coupling position ξ_{ci} is given by

$$h_i(\xi, \xi_{ci}, t) \triangleq f_i(t)\delta(\xi - \xi_{ci}) \tag{2}$$

for an interaction force $f_i(t)$ and

$$h_i(\xi, \xi_{ci}, t) \triangleq g_i(t)\delta'(\xi - \xi_{ci}) \tag{3}$$

for an interaction torque $g_i(t)$, where $\delta'(x)$ is the doublet (derivative of the delta function).

We consider a modal decomposition of the ith structure of the form

$$\chi_i(\xi, t) = \sum_{j=1}^{\infty} q_{ij}(t)\psi_{ij}(\xi), \quad i = 1, \cdots, r, \tag{4}$$

where $q_{ij}(t)$ and $\psi_{ij}(\xi)$ denote modal coordinates and normalized eigenfunctions, respectively, and the double subscript ij denotes the jth mode of the ith substructure. The normalized eigenfunctions $\psi_{ij}(\xi)$ satisfy the orthogonality properties

$$\int_{\Omega_i} \rho_i(\xi)\psi_{ij}(\xi)\psi_{ik}\,d\xi = \delta_{jk}, \quad \int_{\Omega_i} \mathscr{L}_i\psi_{ij}(\xi)\psi_{ik}\,d\xi = \omega_{ij}^2\delta_{jk}, \tag{5}$$

where ω_{ij} is the natural frequency of the jth mode of the ith structure, and δ_{jk} is the Kronecker delta. From (4), (5) and appropriate boundary conditions, it follows that the modal coordinates $q_{ij}(t)$ satisfy the equations of motion

$$\ddot{q}_{ij}(t) + 2\zeta_{ij}\omega_{ij}\dot{q}_{ij}(t) + \omega_{ij}^2 q_{ij}(t) = a_{ij}\tilde{w}_i(t) - b_{ij}v_i(t), \tag{6}$$

where $v_i(t)$ is the coupling interaction and the modal damping term $2\zeta_{ij}\omega_{ij}\dot{q}_{ij}(t)$ is now included. In (6), the modal coefficient a_{ij} is defined by

$$a_{ij} \triangleq \psi_{ij}(\hat{\xi}_i), \tag{7}$$

while

$$b_{ij} \triangleq \psi_{ij}(\xi_{ci}), \qquad v_i(t) \triangleq f_i(t), \tag{8}$$

for force interaction and

$$b_{ij} \triangleq \frac{\partial\psi_{ij}(\xi_{ci})}{\delta\xi}, \qquad v_i(t) \triangleq g_i(t), \tag{9}$$

for torque interaction.

The modal velocity $y_{ij}(t)$ of the jth mode of the ith structure and the

velocity $y_i(t)$ of the ith substructure at the coupling point are given by

$$y_{ij}(t) = b_{ij}\dot{q}_{ij}(t), \tag{10}$$

$$y_i(t) = \sum_{j=1}^{n_i} y_{ij}(t), \tag{11}$$

where n_i is the number of modes of the ith structure in the frequency range of interest. For later use we note that the modal impedance $z_{ij}(s)$, $i = 1, \cdots, r$, $j = 1, \cdots, n_i$, is given by

$$z_{ij}(s) = \frac{s^2 + 2\zeta_{ij}\omega_{ij}s + \omega_{ij}^2}{s}. \tag{12}$$

Our goal is to derive an energy flow model for r interconnected structures represented by (6) and design an energy flow controller to reduce the vibration of a specified substructure. First, we derive two energy flow models by using (6) as the basic equation and then apply the control techniques developed in Kishimoto et al. (1995 b).

3. Energy Flow Modeling: Modal Subsystem Model

First, we obtain the modal subsystem model by considering each mode as a subsystem. Let $w_{ij}(t)$ denote the disturbance force exciting the jth mode of the ith structure, that is,

$$w_{ij}(t) = a_{ij}\tilde{w}_i(t), \quad i = 1, \cdots, r, \quad j = 1, \cdots, n_i, \tag{13}$$

and we assume that the coupling interaction $v_i(t)$ and the structural velocity $y_i(t)$ are related by a coupling transfer function $L(s)$, that is,

$$v_s = L(s)y_s, \tag{14}$$

where $y_s(t) \triangleq [y_1(t) \cdots y_r(t)]^T$ and $v_s(t) \triangleq [v_1(t) \cdots v_r(t)]^T$.

To obtain a feedback representation of the interconnected systems, we define the modal impedance matrix

$$Z_m(s) \triangleq \mathrm{diag}(z_{11}(s), z_{12}(s), \cdots, z_{1n_1}(s), \cdots, z_{r1}(s), \cdots, z_{rn_r}(s)) \tag{15}$$

and the vectors

$$y_m(t) \triangleq [\dot{q}_{11}(t) \cdots \dot{q}_{1n_1}(t) \quad \dot{q}_{21}(t) \cdots \dot{q}_{2n_2}(t) \quad \cdots \quad \dot{q}_{r1}(t) \cdots \dot{q}_{rn_r}(t)]^T, \tag{16}$$

$$w_m(t) \triangleq [w_{11}(t) \cdots w_{1n_1}(t) \quad w_{21}(t) \cdots w_{2n_2}(t) \quad \cdots \quad w_{r1}(t) \cdots w_{rn_r}(t)]^T, \tag{17}$$

$$\tilde{w}(t) \triangleq [\tilde{w}_1(t) \cdots \tilde{w}_r(t)]^T. \tag{18}$$

Note that $w_m(t) = D_m\tilde{w}(t)$, $y_s(t) = E_m^T y_m(t)$ and $v_m(t) = E_m v_s(t)$, where the matrices D_m and E_m are defined by

$$D_m \triangleq \begin{bmatrix} a_{11} & \cdots & a_{1n_1} & 0 & \cdots & 0 & 0 & \cdots & 0 & 0 & \cdots & 0 \\ 0 & \cdots & 0 & a_{21} & \cdots & a_{2n_2} & 0 & \cdots & 0 & 0 & \cdots & 0 \\ \vdots & \vdots & \vdots & \vdots & \vdots & \vdots & \vdots & \vdots & \vdots & \vdots & \vdots & \vdots \\ 0 & \cdots & 0 & 0 & \cdots & 0 & 0 & \cdots & 0 & a_{r1} & \cdots & a_{rn_r} \end{bmatrix}^T, \tag{19}$$

$$E_m \triangleq \begin{bmatrix} b_{11} & \cdots & b_{1n_1} & 0 & \cdots & 0 & 0 & \cdots & 0 & 0 & \cdots & 0 \\ 0 & \cdots & 0 & b_{21} & \cdots & b_{2n_2} & 0 & \cdots & 0 & 0 & \cdots & 0 \\ \vdots & \vdots & \vdots & \vdots & \vdots & \vdots & \vdots & \vdots & \vdots & \vdots & \vdots & \vdots \\ 0 & \cdots & 0 & 0 & \cdots & 0 & 0 & \cdots & 0 & b_{r1} & \cdots & b_{rn_r} \end{bmatrix}^T. \tag{20}$$

With this notation the interconnected system (6) can be expressed as the feedback system shown in Fig. 1, where $u_m(t) \triangleq w_m(t) - v_m(t)$ and the coupling matrix $L_m(s)$ for the modal subsystem model satisfying $v_m = L_m y_m$ is defined by

$$L_m(s) \triangleq E_m L(s) E_m^T. \tag{21}$$

Note that if $L(s)$ is conservative, that is, $L(j\omega) + L^*(j\omega) = 0$, it follows that

$$\begin{aligned} &L_m(j\omega) + L_m^*(j\omega) \\ &\quad = E_m L(j\omega) E_m^T + (E_m L(j\omega) E_m^T)^* \\ &\quad = E_m (L(j\omega) + L^*(j\omega)) E_m^T \\ &\quad = 0, \end{aligned} \tag{22}$$

so that $L_m(s)$ is also conservative. In the same manner if $L(s)$ is dissipative, that is, $L(j\omega) + L^*(j\omega) \geq 0$, then $L_m(s)$ is also dissipative, $L_m(j\omega) + L_m^*(j\omega) \geq 0$. Since now $Z_m(s)$ is strictly positive real it follows from Kishimoto and Bernstein (1995 a) that the feedback system in Fig. 1 is asymptotically stable.

Now we consider three steady-state average energy flows P_{ij}^c, P_{ij}^d and P_{ij}^e, $i = 1, \cdots, r$, $j = 1, \cdots, n_i$ which symbolize

P_{ij}^c = the steady-state average energy flow entering the jth mode of ith structure through the coupling $L_m(s)$,

P_{ij}^d = the steady-state average energy dissipation rate of the jth mode of ith structure,

P_{ij}^e = the steady-state average external power entering the jth mode of ith structure.

To evaluate these steady-state average energy flows consider state-space realizations of $Z_m^{-1}(s)$ and $L(s)$ in Fig. 1 given by

$$\dot{x}_m(t) = A_m x_m(t) + B_m u_m(t), \tag{23}$$

$$y_m(t) = C_m x_m(t), \tag{24}$$

$$\dot{x}_L(t) = A_L(t) x_L(t) + B_L y_s(t), \tag{25}$$

$$v_s(t) = C_L x_L(t), \tag{26}$$

respectively. Since $u_m(t) = w_m(t) - v_m(t) = D_m \tilde{w}(t) - E_m v_s(t)$ and $y_s(t)$

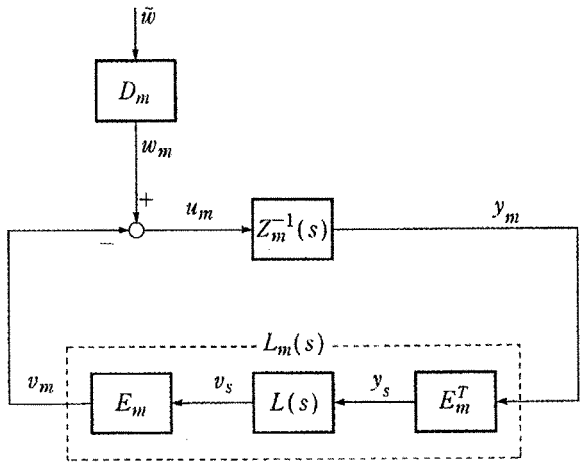

Fig. 1. Feedback representation of modal subsystem model.

$= E_m^T y_m(t)$, the augmented system (23)–(26) is given by

$$\dot{x}_{am}(t) = \tilde{A}x_{am}(t) + \tilde{D}\tilde{w}(t), \tag{27}$$

where

$$x_{am}(t) \triangleq \begin{bmatrix} x_m(t) \\ x_L(t) \end{bmatrix}, \quad \tilde{A} \triangleq \begin{bmatrix} A_m & -B_m E_m C_L \\ B_L E_m^T C_m & A_L \end{bmatrix}, \quad \tilde{D} \triangleq \begin{bmatrix} B_m D_m \\ 0 \end{bmatrix}.$$

Also define C_{m1} and C_{m2} by

$$C_{m1} \triangleq [C_m \quad 0], \quad C_{m2} \triangleq [0 \quad E_m C_L], \tag{28}$$

so that $y_m(t) = C_{m1} x_{am}(t)$ and $v_m(t) = C_{m2} x_{am}(t)$.

Next, we define the diagonal damping matrix

$$C_{md} \triangleq \mathrm{Re}[Z_m(s)], \tag{29}$$

and note that (12) and (15) imply

$$C_{mdiiij} = 2\zeta_{ij}\omega_{ij}, \tag{30}$$

where A_{ijpq} denotes $A_{(n_{ij},n_{pq})}$ and $n_{ij} \triangleq (\sum_{l=1}^{i-1} n_l) + j$. With this notation the steady-state average energy flows P_{ij}^c, P_{ij}^d and P_{ij}^e are given by Kishimoto and Bernstein (1995 a)

$$P_{ij}^c = -\mathscr{E}[\dot{q}_{ij} v_{m(n_{ij})}] = -(C_{m2}\tilde{Q}_m C_{m1}^T)_{ijij}, \tag{31}$$

$$P_{ij}^d = -\mathscr{E}[\dot{q}_{ij} u_{m(n_{ij})}] = -(C_{md} C_{m1} \tilde{Q}_m C_{m1}^T)_{ijij}, \tag{32}$$

$$P_{ij}^e = \mathscr{E}[\dot{q}_{ij} w_{m(n_{ij})}] = \frac{1}{2}(D_m \tilde{D}^T C_{m1}^T)_{ijij}, \tag{33}$$

where $v_{m(n_{ij})}$, $u_{m(n_{ij})}$ and $w_{m(n_{ij})}$ are the n_{ij}th element of $v_m(t)$, $u_m(t)$ and $w_m(t)$, respectively, and the steady-state covariance $\tilde{Q}_m \triangleq \lim_{t\to\infty} \mathscr{E}[x_{am}(t)x_{am}^T(t)]$ satisfies the algebraic Lyapunov equation

$$\tilde{A}\tilde{Q}_m + \tilde{Q}_m\tilde{A}^T + \tilde{D}\tilde{D}^T = 0. \tag{34}$$

As shown in Kishimoto and Bernstein (1995 a) and Kishimoto et al. (1993), P_{ij}^c, P_{ij}^d and P_{ij}^e satisfy

$$P_{ij}^c + P_{ij}^d + P_{ij}^e = 0, \quad i = 1, \cdots, r, \quad j = 1, \cdots, n_i. \tag{35}$$

Furthermore, if $L(s)$ is conservative, then (Kishimoto and Bernstein, 1995 a)

$$\sum_{i=1}^{r}\sum_{j=1}^{n_i} P_{ij}^c = 0, \tag{36}$$

while if $L(s)$ is dissipative, then (Kishimoto and Bernstein, 1995 b)

$$\sum_{i=1}^{r}\sum_{j=1}^{n_i} P_{ij}^c \leq 0. \tag{37}$$

Figure 2 illustrates energy flow among four modes of two interconnected structures.

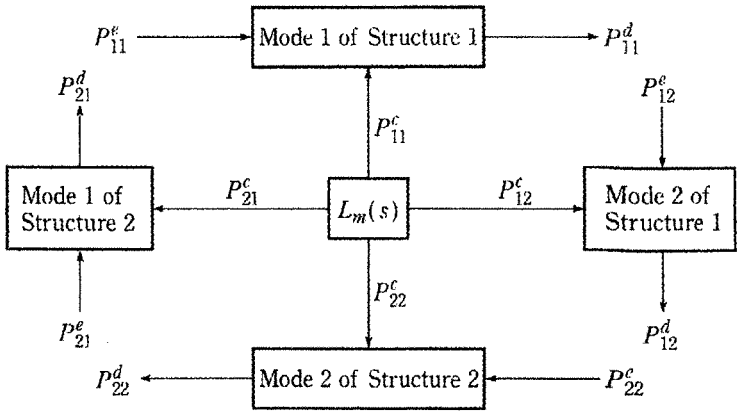

Fig. 2. Energy flow model for two structures and four coupled modes.

4. Energy Flow Modeling: Structural Subsystem Model

Now, we obtain the structural subsystem energy flow model by treating each substructure as a subsystem. In this model, the energy flows are evaluated at the coupling points of the substructures. Hence the total impedance $z_i(s)$ of the ith structure at the coupling point is given by

$$\frac{1}{z_i(s)} = \sum_{j=1}^{n_i} \frac{b_{ij}^2}{z_{ij}(s)} \tag{38}$$

for $i = 1, \cdots, r$. Additionally, by using the fact that the transfer admittance

from the external force $\tilde{w}_i(t)$ at $\hat{\xi}_i$ to the velocity $y_i(t)$ at ξ_{ci} is given by $\sum_{j=1}^{n_i}(a_{ij}b_{ij}/z_{ij}(s))$ (see p.263 in Skudrzyk (1968), it follows that the filter function $T_i(s)$ defined by

$$T_i(s) \triangleq z_i(s)\sum_{j=1}^{n_i}\frac{a_{ij}b_{ij}}{z_{ij}(s)} \tag{39}$$

transforms the external disturbance force $\tilde{w}_i$ at $\hat{\xi}_i$ into the disturbance force w_i at the coupling point ξ_{ci}, that is,

$$w_i = T_i\tilde{w}_i. \tag{40}$$

With this notation (6) can be rewritten as

$$z_i(s)y_i = w_i - v_i, \tag{41}$$

which corresponds to the electrical representation of the interconnected systems shown in Fig. 1 of Kishimoto et al. (1995).

Since $z_i(s)$ is strictly positive real, it follows that

$$c_i(\omega) \triangleq \mathrm{Re}[z_i(j\omega)] > 0, \quad i = 1, \cdots, r, \quad \omega \in \mathscr{R}, \tag{42}$$

where $c_i(\omega)$ is the frequency-dependent resistance or damping. For convenience, define the $r \times r$ diagonal transfer function

$$Z_s(s) \triangleq \mathrm{diag}(z_1(s), \cdots, z_r(s)), \tag{43}$$

and the frequency-dependent resistance or damping matrix

$$C_d(j\omega) \triangleq \mathrm{Re}[Z_s(j\omega)] = \mathrm{diag}(c_1(\omega), \cdots, c_r(\omega)). \tag{44}$$

With this notation the interconnected system in (41) can be expressed as a feedback system in Fig. 3. In Fig. 3, $w_s(t) \triangleq [w_1(t) \cdots w_r(t)]^T$, $u_s(t) \triangleq [u_1(t) \cdots u_r(t)]^T = w_s(t) - v_s(t)$ and $y_s(t)$, $v_s(t)$ and $L(s)$ satisfy (14).

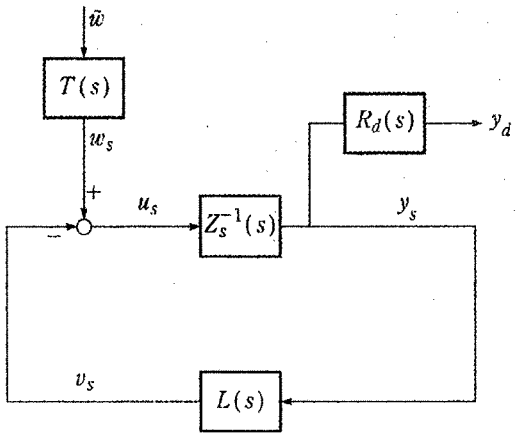

Fig. 3. Feedback representation of structural subsystem model.

Now, we consider the steady-state average energy flow among substructures. In a similar manner to the previous section, the steady-state average energy flows P_i^c, P_i^d and P_i^e are defined for $i = 1, \cdots, r$ by

$$P_i^c \triangleq -\mathscr{E}[y_i(t)v_i(t)], \tag{45}$$

$$P_i^d \triangleq -\mathscr{E}[y_i(t)u_i(t)], \tag{46}$$

$$P_i^e \triangleq \mathscr{E}[y_i(t)w_i(t)], \tag{47}$$

where $u_i(t)$ is the ith element of $u_s(t)$. The meaning of these energy flow quantities corresponds to the meanings of P_{ij}^c, P_{ij}^d and P_{ij}^e in the previous section, respectively, but now P_i^c, P_i^d and P_i^e are the energy flows for the ith substructure and P_i^c is the energy flow through the coupling $L(s)$ in Fig. 3.

In the previous section, we expressed P_{ij}^c, P_{ij}^d, P_{ij}^e in terms of the steady-state covariance $\tilde{Q}_m$ according to the approach in Kishimoto and Bernstein (1995 a) and Kishimoto et al. (1993). In the structural energy flow model, however, the real part $c_i(s)$ of $z_i(s)$, is not constant and the disturbance $w_i(t)$ entering $z_i(s)$ is no longer white noise. Thus, to obtain the steady-state covariance corresponding to $\tilde{Q}_m$ we now introduce two filter transfer function matrices $T(s)$ and $R_d(s)$ as shown in Fig. 3, where the disturbance filter $T(s)$ is defined by

$$T(s) \triangleq \operatorname{diag}(T_1(s), T_2(s), \cdots, T_r(s)), \tag{48}$$

and the stable dissipation filter $R_d(s)$ satisfying (MacMartin and Hall, 1991)

$$R_d(s)R_d^T(-s) = C_d(s). \tag{49}$$

Now, let $Z_s^{-1}(s)$, $T(s)$ and $R_d(s)$ have the realizations

$$\dot{x}_s(t) = A_s x_s(t) + B_s u_s(t), \tag{50}$$

$$y_s(t) = C_s x_s(t), \tag{51}$$

$$\dot{x}_w(t) = A_w x_w(t) + B_w \tilde{w}(t), \tag{52}$$

$$w_s(t) = C_w x_w(t) + D_w \tilde{w}(t), \tag{53}$$

$$\dot{x}_R(t) = A_R x_R(t) + B_R y_s(t), \tag{54}$$

$$y_R(t) = C_R x_R(t) + D_R y_s(t), \tag{55}$$

respectively. By considering the state space model of $L(s)$ given in (25) and (26), the augmented system is given by

$$\dot{x}_{as}(t) = \tilde{A} x_{as}(t) + \tilde{D}\tilde{w}(t), \tag{56}$$

where

$$x_{as}(t) \triangleq \begin{bmatrix} x_s(t) \\ x_w(t) \\ x_R(t) \\ x_L(t) \end{bmatrix}, \quad \tilde{A} \triangleq \begin{bmatrix} A_s & B_s C_w & 0 & -B_s C_L \\ 0 & A_w & 0 & 0 \\ B_R C_s & 0 & A_R & 0 \\ B_L C_s & 0 & 0 & A_L \end{bmatrix}, \quad \tilde{D} \triangleq \begin{bmatrix} B_s D_w \\ B_w \\ 0 \\ 0 \end{bmatrix}.$$

Furthermore, define

$$C_{s1} \triangleq [C_s \quad 0 \quad 0 \quad 0],$$

$$C_{s2} \triangleq [0 \quad 0 \quad 0 \quad C_L],$$

$$C_{sd} \triangleq [D_R C_s \quad 0 \quad C_R \quad 0],$$

so that $y_s(t) = C_{s1} x_{as}(t)$, $v(t) = C_{s2} x_{as}(t)$ and $y_R(t) = C_{sd} x_{as}(t)$.

With the above notation, P_i^c and P_i^d are given by Kishimoto and Bernstein (1995 a)

$$P_i^c = -(C_{s2} \tilde{Q}_s C_{s1}^T)_{(i,i)}, \tag{57}$$

$$P_i^d = -(C_{sd} \tilde{Q}_s C_{sd}^T)_{(i,i)}, \tag{58}$$

where the steady-state covariance $\tilde{Q}_s \triangleq \lim_{t \to \infty} \mathcal{E}[x_{as}(t) x_{as}^T(t)]$ satisfies

$$0 = \tilde{A} \tilde{Q}_s + \tilde{Q}_s \tilde{A}^T + \tilde{D} \tilde{D}^T. \tag{59}$$

As in the modal subsystem energy flow model, P_i^c, P_i^d and P_i^e satisfy

$$P_i^c + P_i^d + P_i^e = 0. \tag{60}$$

Furthermore if $L(s)$ is conservative, then

$$\sum_{i=1}^{r} P_i^c = 0, \tag{61}$$

while if $L(s)$ is dissipative, then

$$\sum_{i=1}^{r} P_i^c \leq 0. \tag{62}$$

These results are illustrated in Fig. 3 of Kishimoto et al. (1995 b) for the case $r = 3$.

In the following four sections, we consider two types of energy flow control techniques introduced from Kishimoto et al. (1995 b) and design strictly positive real controllers by using the LQG positive real control approach explained in Sec. 3 of Kishimoto et al. (1995 b).

Note that in Kishimoto et al. (1995 b) only one structure was considered. The following sections, which consider multiple coupled substructures, will allow us to contrast the modal and structural subsystem models.

5. Design of an Energy Flow Controller as an Additional Subsystem: Modal Subsystem Model

In this section, we consider a control problem involving $r-1$ structures interconnected by a stiffness (lossless) coupling and design the controller as an additional subsystem as discussed in Sec. 4 of Kishimoto et al. (1995 b).

Now, we connect the single-input single-output controller $z_c^{-1}(s)$ to the structures $Z_m^{-1}(s)$ whose state space model is given by (23) and (24). The additional subsystem, that is, the controller $z_c^{-1}(s)$ is assumed to be expressed by

$$\dot{x}_c(t) = A_c x_c(t) + B_c y(t), \tag{63}$$

$$u(t) = C_c x_c(t), \tag{64}$$

where $u(t)$ and $y(t)$ are scalars and we now assume that the disturbance does not directly enter into the controller $z_c^{-1}(s)$. Then the augmented feedback representation of the feedback system corresponding to Fig. 1 is shown in Fig. 4. In Fig. 4,

$$E_a \triangleq \begin{bmatrix} E_m & 0 \\ 0 & 1 \end{bmatrix}, \quad D_a \triangleq \begin{bmatrix} D_m \\ 0 \end{bmatrix},$$

where D_m and E_m are defined by (19), (20), respectively.

As shown in Fig. 4, the admittance matrix corresponding to $Z_m^{-1}(s)$ in Fig. 1 is now comprised of $Z_m^{-1}(s)$ and $z_c^{-1}(s)$. In this case, the augumented vectors $y_{am}(t)$, $u_{am}(t)$, $w_{am}(t)$ and $w_a(t)$ in Fig. 4 are defined by

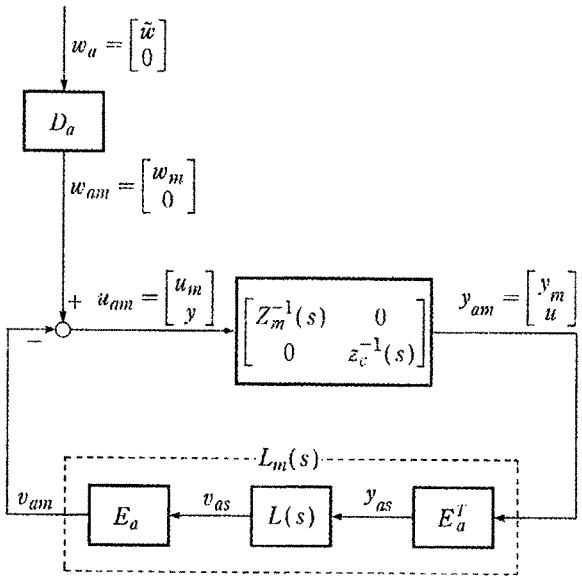

Fig. 4. Feedback representation of plant and controller (Modal subsystem model).

$$y_{am}(t) \triangleq \begin{bmatrix} y_m(t) \\ u(t) \end{bmatrix}, \qquad u_{am}(t) \triangleq \begin{bmatrix} u_m(t) \\ y(t) \end{bmatrix},$$

$$w_{am}(t) \triangleq \begin{bmatrix} w_m(t) \\ 0 \end{bmatrix}, \qquad w_a(t) \triangleq \begin{bmatrix} \tilde{w}(t) \\ 0 \end{bmatrix},$$

respectively.

On the other hand, the stiffness coupling $L(s)$ is now expressed by

$$L(s) = \frac{1}{s} C_L, \tag{65}$$

where the symmetric matrix $C_L \in \mathscr{R}^{r \times r}$ is partitioned as

$$C_L \triangleq \begin{bmatrix} C_{L_{11}} & C_{L_{12}} \\ C_{L_{12}}^T & C_{L_{22}} \end{bmatrix}. \tag{66}$$

In the same manner as Sec. 4 of Kishimoto et al. (1995 b), we define the position vectors $y_{pm}(t) \triangleq \int y_m(t)dt = C_{pm} x_m(t)$ for $Z_m^{-1}(s)$ and a scalar state $x_{pc}(t)$ by

$$\dot{x}_{pc}(t) \triangleq u(t), \tag{67}$$

for the controller $z_c^{-1}(s)$ so that the output vector v_{am} of the stiffness coupling $L_m(s)$ is given by

$$v_{am} = E_a \frac{1}{s} C_L E_a^T y_{am} = E_a C_L \begin{bmatrix} C_{pm} E_m^T x_m \\ x_{pc} \end{bmatrix}. \tag{68}$$

By using (63)–(68), the feedback system shown in Fig. 4 is expressed as

$$\dot{x}_{am}(t) = \tilde{A} x_{am}(t) + \tilde{D} \tilde{w}(t), \tag{69}$$

where

$$\tilde{A} \triangleq \begin{bmatrix} A_m - B_m E_m C_{L_{11}} E_m^T C_{pm} & -B_m E_m C_{L_{12}} & 0 \\ 0 & 0 & C_c \\ -B_c C_{L_{12}}^T E_m^T C_{pm} & -B_c C_{L_{22}} & A_c \end{bmatrix},$$

$$\tilde{D} \triangleq \begin{bmatrix} B_m D_m \\ 0 \\ 0 \end{bmatrix}, \quad x_{am}(t) \triangleq \begin{bmatrix} x_m(t) \\ x_{pc}(t) \\ x_c(t) \end{bmatrix}.$$

Furthermore, define

$$C_{am} \triangleq [C_m \quad 0 \quad 0], \tag{70}$$

so that $y_{am}(t) = C_{am} x_{am}(t)$.

We now determine (A_c, B_c, C_c) by means of the LQG positive real approach. By defining

$$x(t) \triangleq \begin{bmatrix} x_m(t) \\ x_{pc}(t) \end{bmatrix}, \quad A \triangleq \begin{bmatrix} A_m - B_m E_m C_{L11} E_m^T C_{pm} & -B_m E_m C_{L12} \\ 0 & 0 \end{bmatrix},$$

$$B \triangleq [0 \cdots 0 \quad 1]^T, \quad C \triangleq [-C_{L21} E_m^T C_{pm} \quad -C_{L22}], \quad D_1 \triangleq \begin{bmatrix} B_m D_m \\ 0 \end{bmatrix},$$

it follows that $\tilde{A}$ and $\tilde{D}$ in (69) can be expressed as

$$\tilde{A} = \begin{bmatrix} A & BC_c \\ B_c C & A_c \end{bmatrix}, \quad \tilde{D} = \begin{bmatrix} D_1 \\ B_c D_2 \end{bmatrix}, \tag{71}$$

where D_2 in $\tilde{D}$ represents fictitious measurement noise required by the LQG approach.

Now the controller is required to reduce the vibration of a specified substructure. For this purpose, we define the total energy flow through the coupling to all n_i modes of the ith structure $\mathscr{P}_i^c$ given by $\mathscr{P}_i^c = \sum_{j=1}^{n_i} P_{ij}^c$, while $\mathscr{P}_i^d$ and $\mathscr{P}_i^e$ defined by

$$\mathscr{P}_i^d \triangleq \sum_{j=1}^{n_i} P_{ij}^d, \quad \mathscr{P}_i^e \triangleq \sum_{j=1}^{n_i} P_{ij}^e$$

have a similar interpretation (Kishimoto et al., 1995 a). Furthermore, from (35), it follows that

$$\mathscr{P}_i^c + \mathscr{P}_i^e = -\mathscr{P}_i^d. \tag{72}$$

Since $\mathscr{P}_i^c$ represents energy flow entering the ith structure through the coupling and $\mathscr{P}_i^e$ represents external energy flow entering the ith structure, it follows that the left hand side of (72) represents the total energy flow entering the ith structure. Hence by minimizing $-\mathscr{P}_i^d$, we can minimize the total energy flow entering the ith structure and as a result we can reduce the vibration of the ith structure.

Now defining the augmented diagonal matrix C_{am}

$$C_{am} \triangleq \begin{bmatrix} C_{md} & 0 \\ 0 & 0 \end{bmatrix}, \tag{73}$$

where C_{md} is defined (29), and using (72) with (32) and (69) yields

$$\begin{aligned} -\mathscr{P}_i^d &= \sum_{j=1}^{n_i} [C_{am} C_{am} \tilde{Q}_{am} C_{am}]_{ijij} \\ &= \mathrm{tr}\left[\sum_{j=1}^{n_i} [e_{n_{ij}}^T C_{am} C_{am} \mathscr{E}[x_{am} x_{am}^T] C_{am} e_{n_{ij}}] \right] \\ &= \mathscr{E}\left[\mathrm{tr}\left[x_{am}^T C_{am}^T \left(\sum_{j=1}^{n_i} e_{n_{ij}} e_{n_{ij}}^T C_{am} \right) C_{am} x_{am} \right] \right] \\ &= \mathscr{E}[x_{am}^T C_{am}^T \tilde{C}_1 C_{am} x_{am}], \end{aligned}$$

where the steady-state covariance $\tilde{Q}_{am} \triangleq \lim_{t \to \infty} \mathscr{E}[x_{am}(t) x_{am}^T(t)]$ satisfies

$$0 = \tilde{A}\tilde{Q}_{am} + \tilde{Q}_{am}\tilde{A}^T + \tilde{D}\tilde{D}^T \tag{74}$$

and

$$\tilde{C}_1 \triangleq \sum_{j=1}^{n_i} e_{n_{ij}} e_{n_{ij}}^T C_{am}. \tag{75}$$

Thus, letting the performance variables have the form

$$z(t) = E_1 x(t) + E_2 u(t), \tag{76}$$

it follows that E_1 is given by

$$E_1 = \tilde{C}_1^{\frac{1}{2}} C_{am}. \tag{77}$$

As shown in Kishimoto et al. (1995 b) the plant (A, B, C) is positive real so that the results in Sec. 3 of Kishimoto et al. (1995) can be used to determine a positive real compensator $z_c^{-1}(s)$.

6. Design of an Energy Flow Controller as an Additional Subsystem: Structural Subsystem Model

Now, we design an energy flow controller based on the structural subsystem model. In this case, the dynamics of the dissipation filter $R_d(s)$ and the disturbance filter $T(s)$ must be included in the control design.

As in the previous section by augmenting the vectors and matrices in Fig. 3 we obtain Fig. 5 as the feedback representation of the structural subsystem energy flow model. In Fig. 5,

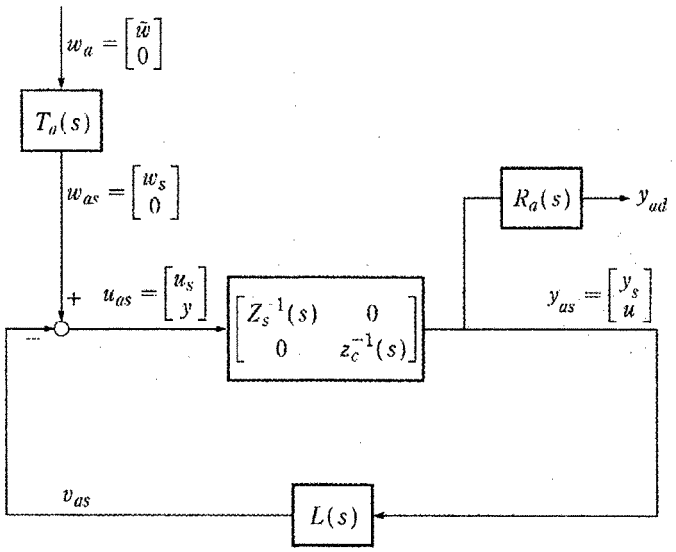

Fig. 5. Feedback representation of plant and controller (Structural subsystem model).

$$y_{as}(t) \triangleq \begin{bmatrix} y_s(t) \\ u(t) \end{bmatrix}, \quad u_{as}(t) \triangleq \begin{bmatrix} u_s(t) \\ y(t) \end{bmatrix}, \quad w_{as}(t) \triangleq \begin{bmatrix} w_s(t) \\ 0 \end{bmatrix},$$

$$T_a(s) \triangleq \begin{bmatrix} T(s) & 0 \\ 0 & 0 \end{bmatrix}, \quad R_a(s) \triangleq \begin{bmatrix} R_d(s) & 0 \\ 0 & 0 \end{bmatrix},$$

where $T(s)$ and $R_d(s)$ are defined by (48) and (49), respectively. As shown in Fig. 5 the admittance matrix corresponding to $Z_s^{-1}(s)$ in Fig. 3 is now comprised of $Z_s^{-1}(s)$ and $z_c^{-1}(s)$ whose state space model are given by (50) and (51), (63) and (64), respectively.

Furthermore, by defining $y_{ps}(t) \triangleq \int y_s(t)dt = C_{ps}x_s(t)$ for the structural subsystem energy flow model and using a scalar state $x_{pc}(t)$ in (67) the output vector $v_{as}(t)$ of the stiffness coupling $L(s)$ is given by

$$v_{as}(t) = \frac{1}{s} C_L y_{as}(t) = C_L \begin{bmatrix} C_{ps}x(t) \\ x_{pc}(t) \end{bmatrix}. \tag{78}$$

Then the state space model of the feedback system shown in Fig. 5 is given by

$$\dot{x}_{as}(t) = \tilde{A}x_{as}(t) + \tilde{D}\tilde{w}(t), \tag{79}$$

where

$$\tilde{A} \triangleq \begin{bmatrix} A_s - B_s C_{L_{11}} C_{ps} & B_s C_w & 0 & -B_s C_{L_{12}} & 0 \\ 0 & A_w & 0 & 0 & 0 \\ B_R C_s & 0 & A_R & 0 & 0 \\ 0 & 0 & 0 & 0 & C_c \\ -B_c C_{L_{21}} C_{ps} & 0 & 0 & -B_c C_{L_{22}} & A_c \end{bmatrix},$$

$$\tilde{D} \triangleq \begin{bmatrix} B_s D_w \\ B_w \\ 0 \\ 0 \\ 0 \end{bmatrix}, \quad x_{as}(t) \triangleq \begin{bmatrix} x_s(t) \\ x_w(t) \\ x_R(t) \\ x_{pc}(t) \\ x_c(t) \end{bmatrix}.$$

Furthermore, define

$$C_{ad} \triangleq [D_R C_s \quad 0 \quad C_R \quad 0 \quad 0], \tag{80}$$

so that $y_{ad}(t) = C_{ad}x_{as}(t)$.

As in the previous section by defining

$$A \triangleq \begin{bmatrix} A_s - B_s C_{L11} C_{ps} & B_s C_w & 0 & -B_s C_{L12} \\ 0 & A_w & 0 & 0 \\ B_R C_s & 0 & A_R & 0 \\ 0 & 0 & 0 & 0 \end{bmatrix},$$

$$B \triangleq [0 \cdots 0 \quad 1]^T,$$

$$C \triangleq [-C_{L21}C_{ps} \quad -C_{L22}]$$

$$D_1 \triangleq \begin{bmatrix} B_s D_w \\ B_w \\ 0 \\ 0 \end{bmatrix},$$

it follows that $\tilde{A}$ and $\tilde{D}$ in (79) are of the form of (71). Thus, (79) can be interpreted as an LQG control problem (Kishimoto et al., 1995 b).

Now, we choose E_1 in (76) by using energy balance at each subsystem. From (58) and (60), it follows that

$$P_i^c + P_i^e = -P_i^d = (C_{ad}\tilde{Q}_{as}C_{ad}^T)_{(i,i)}, \tag{81}$$

where the steady-state covariance $\tilde{Q}_{as} \triangleq \lim_{t\to\infty} \mathscr{E}[x_{as}(t)x_{as}^T(t)]$ satisfies

$$0 = \tilde{A}\tilde{Q}_{as} + \tilde{Q}_{as}\tilde{A}^T + \tilde{D}\tilde{D}^T. \tag{82}$$

In a similar manner to the previous section, by minimizing $-P_i^d = (C_{ad}\tilde{Q}_{as}C_{ad}^T)_{(i,i)}$, we can minimize the total energy flow entering the ith structure and thus reduce the vibration of the ith structure. Since now

$$-P_i^d = (C_{ad}\tilde{Q}_{as}C_{ad}^T)_{(i,i)} = \mathscr{E}[x_{as}^T C_{ad}^T e_i e_i^T C_{ad} x_{as}],$$

it follows that

$$E_1 = e_i^T C_{ad}. \tag{83}$$

As in the previous section, since the plant (A, B, C) is positive real, a positive real compensator $G_c(s) = z_c^{-1}(s)$ can be obtained by using the results in Sec. 3 of Kishimoto et al. (1995 b).

7. Design of an Energy Flow Controller as a Dissipative Coupling: Modal Subsystem Model

As a second application of the results of Kishimoto et al. (1995 b), we now consider the interconnection of two structures by means of an interstitial relative force controller. This problem can be viewed as an extension of the results of Sec. 6 of Kishimoto et al. (1995 b). Let $Z_m^{-1}(s)$ and $G_c(s)$ represent the transfer functions of the two uncoupled strictly positive real systems and the controller, respectively. In the modal subsystem model, the state space model of $Z_m^{-1}(s)$ is given by (23), (24), where $G_c(s)$ has the state space realization

$$\dot{x}_c(t) = A_c x_c(t) + B_c y(t), \tag{84}$$

$$u(t) = C_c x_c(t), \tag{85}$$

where $u(t)$ and $y(t)$ are scalars.

To obtain the relative velocity $y(t)$ from $y_s(t)$ and the coupling force $v(t)$ from $u(t)$, we define $\tilde{B}$ as

$$\tilde{B} \triangleq \begin{bmatrix} 1 \\ -1 \end{bmatrix}. \tag{86}$$

With $\tilde{B}$ given by (86), the feedback systems can be expressed as in Fig. 6, where

$$L(s) \triangleq -\tilde{B}G_c(s)\tilde{B}^T \tag{87}$$

and

$$L_m(s) \triangleq -E_m\tilde{B}G_c(s)\tilde{B}^T E_m^T. \tag{88}$$

If $G_c(s)$ satisfies

$$G_c(s) + G_c^*(s) < 0, \quad \mathrm{Re}[s] > 0, \tag{89}$$

then, for $\mathrm{Re}[s] > 0$,

$$\begin{aligned} &L(s) + L^*(s) \\ &\quad = -\tilde{B}G_c(s)\tilde{B}^T - [\tilde{B}G_c(s)\tilde{B}^T]^* \\ &\quad = -\tilde{B}[G_c(s) + G_c^*(s)]\tilde{B}^T \\ &\quad \geq 0, \end{aligned} \tag{90}$$

which implies that

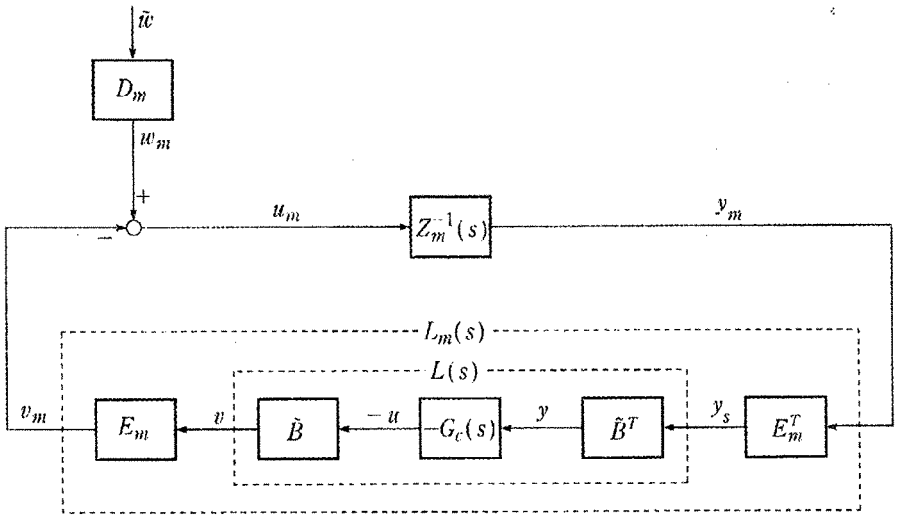

Fig. 6. Feedback representation of coupled system (Modal subsystem model).

$$L_m(s) + L_m^*(s) \geq 0, \quad \mathrm{Re}[s] > 0. \tag{91}$$

Thus, the coupling $L(s)$ and $L_m(s)$ serve as dissipative controllers which control energy flow between the structures.

From (84), (85) and (87),

$$L(s) \sim \left[\begin{array}{c|c} A_c & B_c \tilde{B}^T \\ \hline -\tilde{B}C_c & 0 \end{array}\right],$$

then by comparing the state space model of $L_m(s)$ given by (25) and (26) we obtain

$$A_L = A_c, \quad B_L = B_c \tilde{B}^T, \quad C_L = -\tilde{B}C_c.$$

By substituting these A_L, B_L and C_L into (27) we obtain

$$\dot{x}_{am}(t) = \tilde{A}x_{am}(t) + \tilde{D}\tilde{w}(t), \tag{92}$$

where

$$x_{am}(t) \triangleq \left[\begin{array}{c} x_m(t) \\ x_c(t) \end{array}\right],$$

$$\tilde{A} \triangleq \left[\begin{array}{cc} A_m & B_m E_m \tilde{B} C_c \\ B_c \tilde{B}^T E_m^T C_m & A_c \end{array}\right], \quad \tilde{D} \triangleq \left[\begin{array}{c} B_m D_m \\ 0 \end{array}\right].$$

Define

$$\tilde{C}_{am} \triangleq [C_{md} \quad 0], \tag{93}$$

so that $y_m(t) = \tilde{C}_{am}x_{am}(t)$.

By defining $A \triangleq A_m$, $B \triangleq B_m E_m \tilde{B}$ and $C \triangleq \tilde{B}^T E_m^T C_m$, $\tilde{A}$ in (92) is of the form of (71) so that (92) can be interpreted as an LQG control problem.

As considered in the previous section we minimize $-\mathscr{P}_1^d$, while E_1 in (76) can be obtained by

$$E_1 = \tilde{C}_2^{\frac{1}{2}} \tilde{C}_{am}, \tag{94}$$

where

$$\tilde{C}_2 \triangleq \sum_{j=1}^{n_i} e_{n_{ij}} e_{n_{ij}}^T C_m. \tag{95}$$

8. Design of an Energy Flow Controller as a Dissipative Coupling: Structural Subsystem Model

In the same manner as the previous section, we now design an interstitial relative force controller based on the structural subsystem model.

Now, the state space model of $Z_s^{-1}(s)$ is given by (50), (51) and by defining the controller $G_c(s)$ in (84) and (85) and $\tilde{B}$ in (86) we obtain the feedback

system shown in Fig. 7. By substituting A_L, B_L and C_L obtained in the previous section into (56) the augmented state space model shown in Fig. 7 can be obtained as

$$\dot{x}_{as}(t) = \tilde{A}x_{as}(t) + \tilde{D}\tilde{w}(t), \tag{96}$$

where

$$x_{as}(t) \triangleq \begin{bmatrix} x_s(t) \\ x_w(t) \\ x_R(t) \\ x_c(t) \end{bmatrix}, \quad \tilde{A} \triangleq \begin{bmatrix} A_s & B_s C_w & 0 & B_s \tilde{B} C_c \\ 0 & A_w & 0 & 0 \\ B_R C_s & 0 & A_R & 0 \\ B_c \tilde{B}^T C_s & 0 & 0 & A_c \end{bmatrix}, \quad \tilde{D} \triangleq \begin{bmatrix} B_s D_w \\ B_w \\ 0 \\ 0 \end{bmatrix}.$$

Furthermore, define

$$\tilde{C}_{ad} \triangleq [D_R C_s \quad 0 \quad C_R \quad 0], \tag{97}$$

so that $y_d(t) = \tilde{C}_{ad} x_{as}(t)$.

By defining

$$A \triangleq \begin{bmatrix} A_s & B_s C_w & 0 \\ 0 & A_w & 0 \\ B_R C_s & 0 & A_R \end{bmatrix}, \quad B \triangleq \begin{bmatrix} B_s \tilde{B} \\ 0 \\ 0 \end{bmatrix}, \quad C \triangleq [\tilde{B}^T C_s \quad 0 \quad 0],$$

then (96) is of the form (71) so that LQG control can be applied.

As considered in the previous sections we minimize $-P_1^d$, and as a result E_1 in (76) is given by

$$E_1 = e_1^T \tilde{C}_{ad}. \tag{98}$$

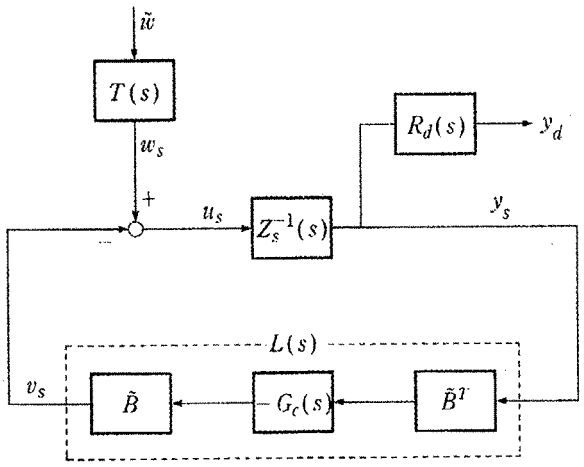

Fig. 7. Feedback representation of coupled system (Structural subsystem model).

As in the previous section the strictly positive real controller $-G_c(s)$ can be obtained by the LQG positive real control approach.

9. Example

To examine the effectiveness of the controllers discussed in the previous sections we consider two examples involving Bernoulli-Euler beams.

Example 1. First, we design an energy flow controller as an additional subsystem for the three simply supported uniform Bernoulli-Euler beams shown in Fig. 8. The beams are of lengths L_1, L_2, L_3, mass densities ρ_1, ρ_2, ρ_3, and bending stiffnesses $E_1 I_{A1}$, $E_2 I_{A2}$, $E_3 I_{A3}$, respectively. Each beam is coupled by the rotational springs K_{12}, K_{23}, K_{13} and subjected to normalized white noise disturbance $\tilde{w}_i(t)$, $i = 1, 2, 3$, with unit intensity applied at $\hat{\xi}_i$. Furthermore, each beam is coupled with the controller by the rotational springs K_{1c}, K_{2c} and K_{3c} at $\xi_{ci} = 0$, $i = 1, 2, 3$.

Since now the coupling interaction is a torque, we consider $h_i(\xi_i, \xi_{c,i}, t)$ in (3), where $g_i(t)$ is given by Crandall and Lotz (1971) and Davies (1972)

$$g_i(t) = \sum_{\substack{m=1 \\ m \neq i}}^{3} K_{im} \left(\frac{\partial \chi_m(\xi_{c_m}, t)}{\partial \xi} - \frac{\partial \chi_i(\xi_{c_i}, t)}{\partial \xi} \right). \tag{99}$$

Furthermore, by considering the boundary conditions

$$\chi_i(\xi, t)|_{\xi=0,L_i} = 0, \quad E_i I_{Ai} \frac{\partial^2 \chi_i(\xi, t)}{\partial \xi^2}\bigg|_{\xi=0,L_i} = 0, \quad i = 1, 2, 3,$$

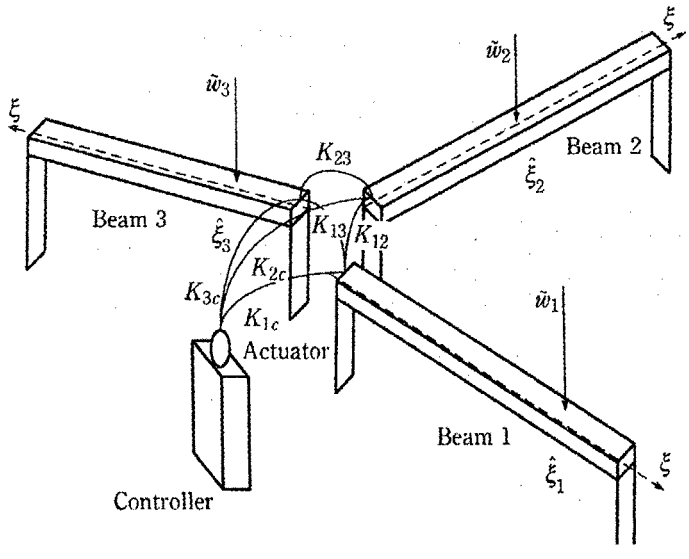

Fig. 8. Three coupled beams and controller.

we obtain the wave number k_{ij}, the natural frequency ω_{ij} and the eigenfunctions $\psi_{ij}(\xi)$ as

$$k_{ij} = \frac{j\pi}{L_i}, \quad \omega_{ij} = k_{ij}^2 \left(\frac{E_i I_{Ai}}{\rho_i} \right)^{\frac{1}{2}}, \quad \psi_{ij}(\xi) = \sqrt{\frac{2}{\rho_i L_i}} \sin k_{ij} \xi,$$
$$i = 1, 2, 3, \quad j = 1, 2, \cdots, n_i .$$

Thus, a_{ij} and b_{ij} in (6) are now given by $a_{ij} = \psi_{ij}(\hat{\xi}_i)$ and $b_{ij} = \sqrt{2} k_{ij}$.

Now, we consider the first three modes of each beam, that is, $n_1 = n_2 = n_3 = 3$ and let $L_1 = \pi$, $L_2 = \pi/\sqrt{1.5}$, $L_3 = \pi/\sqrt{2}$, $\rho_i L_i = 1$ and $E_i I_{Ai} = \rho_i$ for $i = 1, 2, 3$, so that

$$\omega_{1j} = j^2, \quad \omega_{2j} = 1.5j^2, \quad \omega_{3j} = 2j^2, \quad \psi_{ij}(\xi) = \sqrt{2} \sin k_{ij} \xi, \quad i, j = 1, 2, 3 .$$

Let $\zeta_{1j} = 0.01$, $\zeta_{2j} = 0.02$, $\zeta_{3j} = 0.03$, $j = 1, 2, 3$, $K_{12} = 0.1$, $K_{23} = 0.2$, $K_{13} = 0.3$, $K_{1c} = 1$, $K_{2c} = 2$, $K_{3c} = 3$, $\hat{\xi}_1 = 1.5$, $\hat{\xi}_2 = 1.0$ and $\hat{\xi}_3 = 0.5$.

To reduce the vibration of the ith beam, $i = 1, 2, 3$, we design six controllers. Controllers 1, 2 and 3 are designed by the modal subsystem model, which minimizes $-\mathscr{P}_1^d$, $-\mathscr{P}_2^d$ and $-\mathscr{P}_3^d$, respectively, while Controllers 4, 5 and 6 are designed by the structural subsystem model, which minimizes $-P_1^d$, $-P_2^d$ and $-P_3^d$, respectively. The resulting energy flow diagrams are illustrated in Figs. 9 and 10 for the modal subsystem model and the structural subsystem model, respectively, where OL denotes the open-loop system and G_{ci} represents Controller i. Figures 9 and 10 show that each controller absorbs energy from all of the beams and reduces the energy dissipation from each beam. For example, the energy flow entering beams 2 and 3 in the open loop system is reversed by controllers. Furthermore, $\mathscr{P}_i^e$, $i = 1, 2, 3$, in Fig. 9 does not change even after Controllers 1–3 are inserted, while P_i^e, $i = 1, 2, 3$, in Fig. 10 is decreased after Controllers 4–6 are inserted. This fact can be explained as follows. Since the disturbance force entering the subsystem $Z_m^{-1}(s)$, $w_{ij}(t)$, has a constant spectral density it follows that the entering energy flow P_{ij}^e is constant as explained in Kishimoto et al. (1995 b). Thus, Controllers 1–3 do not change $\mathscr{P}_i^e$, $i = 1, 2, 3$. From (72), this fact implies that in the modal subsystem model the performance index minimizing $-\mathscr{P}_i^d$ can be interpreted as maximizing $-\mathscr{P}_i^c$, that is, Controllers 1–3 maximize the energy flow from the specified beam through the coupling as considered in Kishimoto et al. (1995 b). On the other hand, in the structural subsystem model the spectral density of the disturbance force $w_i(t)$ entering the subsystem $Z_s^{-1}(s)$ is no longer constant due to the disturbance filter $T(s)$. Thus, the Controllers 4–6 change the entering energy flow by the disturbance, P_i^e, $i = 1, 2, 3$, and minimize the total energy flow entering the ith beam, $P_i^c + P_i^e$.

To examine the reduction of modal energy by these controllers we define the total steady-state modal energy by

$$\mathscr{E}_i \triangleq \sum_{j=1}^{3} \left(\frac{1}{2} \mathscr{E}[\dot{q}_{ij}^2(t)] + \frac{1}{2} \omega_{ij}^2 \mathscr{E}[q_{ij}^2(t)] \right), \quad i = 1, 2, 3, \qquad (100)$$

which is the steady-state vibrational energy of the ith beam in the absence of

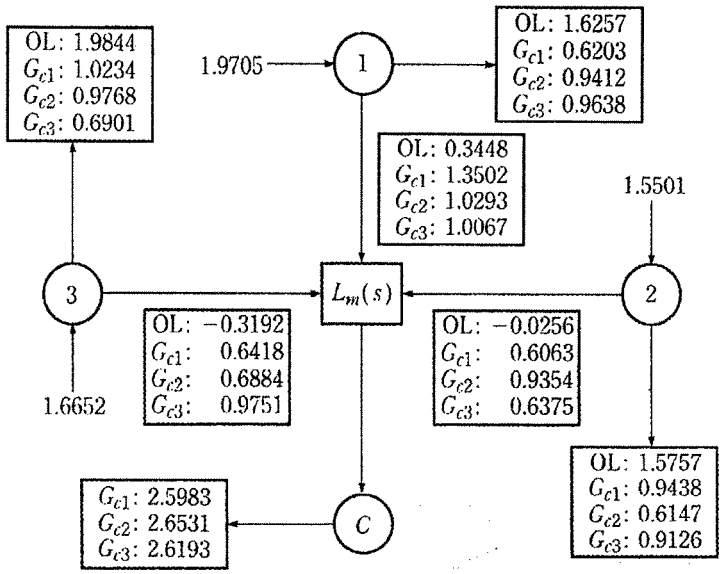

Fig. 9. Energy flow among beams for the open-loop system and for the closed-loop system with controllers G_{c1}, G_{c2} and G_{c3} based on the modal subsystem model.

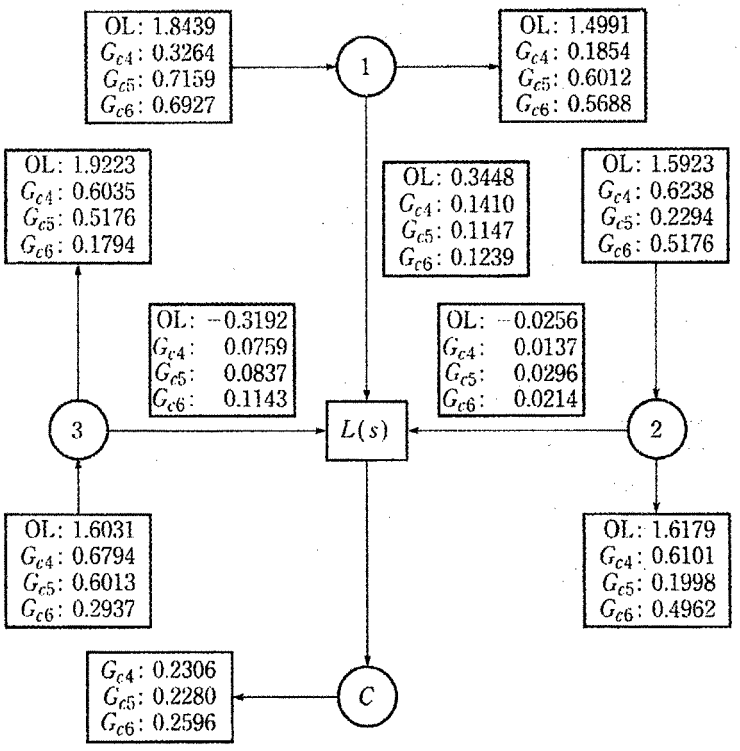

Fig. 10. Energy flow among beams for the open-loop system and for the closed-loop system with controllers G_{c4}, G_{c5} and G_{c6} based on the structural subsystem model.

modal correlation. Table 1 shows that each controller successfully reduces the stored energy $\mathscr{E}_i$ and that the energy flow controllers based on the structural subsystem model, Controllers 4–6, shows better performance compared with Controllers 1–3 based on the modal subsystem model. For example, Controller 1 reduces the modal energy of beam 1 to 39.32 percent of its open-loop value, while Controller 4 reduces it to 31.09 percent. Gain and phase plots of Controllers 1–3, shown in Fig. 11, show that each controller has a gain peak near the coupled natural frequencies of each beam. For example, Controller 1 has a gain peak near $\omega = 2.4$, 4.4, 9.4 [rad/sec.] of Beam 1. These controllers are strictly positive real since their phase plots lie in the range $(-90°, 90°)$. The gain and phase plots for Controllers 4–6 have similar features.

Table 1. Steady-state modal energy for three beams coupled by rotational springs

Modal energy	Open-loop	Controller 1	Controller 2	Controller 3
$\mathscr{E}_1$	4.3697	1.7182 (39.32[%])	2.6760 (61.24[%])	2.5462 (58.27[%])
$\mathscr{E}_2$	2.8609	1.7105 (59.79[%])	1.0763 (37.62[%])	1.7174 (60.03[%])
$\mathscr{E}_3$	1.4236	0.8881 (62.38[%])	0.9034 (63.46[%])	0.4607 (32.36[%])
Modal energy	Open-loop	Controller 4	Controller 5	Controller 6
$\mathscr{E}_1$	4.3697	1.3585 (31.09[%])	2.6201 (59.96[%])	2.5056 (57.34[%])
$\mathscr{E}_2$	2.8609	1.5858 (55.43[%])	0.8688 (30.37[%])	1.6015 (55.98[%])
$\mathscr{E}_3$	1.4236	0.8295 (58.27[%])	0.8842 (62.11[%])	0.3892 (27.34[%])

Example 2. Now we design an energy flow controller to serve as a dissipative coupling for two uniform cantilever beams as shown in Fig. 12. The beams are of lengths L_1, L_2, mass densities ρ_1, ρ_2, and bending stiffnesses $E_1 I_{A1}$, $E_2 I_{A2}$, respectively. Each beam is subjected to mutually uncorrelated white noise disturbances $\tilde{w}_i(t)$, $i = 1, 2$, with unit intensity applied at $\hat{\xi}_i$ and with control force from the coupling controller $f_c(t)$ applied at ξ_{ci}.

Since a force actuator is used, we view the force as a coupling interaction. Thus, in (2), $f_1(t) = f_c(t)$ and $f_2(t) = -f_c(t)$. By considering the boundary conditions

$$\chi_i(\xi, t)|_{\xi=0} = 0, \quad \left.\frac{\partial \chi_i(\xi, t)}{\partial \xi}\right|_{\xi=0} = 0, \quad \left.\frac{\partial^2 \chi_i(\xi, t)}{\partial \xi^2}\right|_{\xi=L_i} = 0,$$

$$\left.\frac{\partial^3 \chi_i(\xi, t)}{\partial \xi^3}\right|_{\xi=L_i} = 0, \quad i = 1, 2,$$

we obtain the natural frequency and eigenfunctions as Norton (1989)

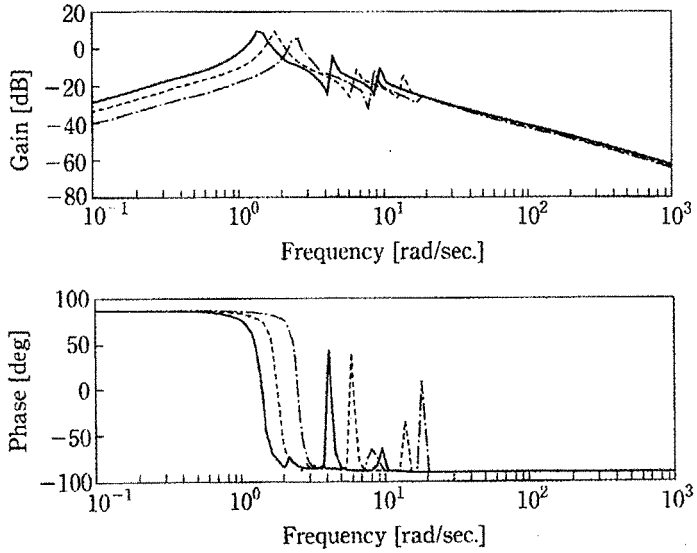

Fig. 11. Magnitude and phase of controllers G_{c1} (solid), G_{c2} (dashed), G_{c3} (dash-dot).

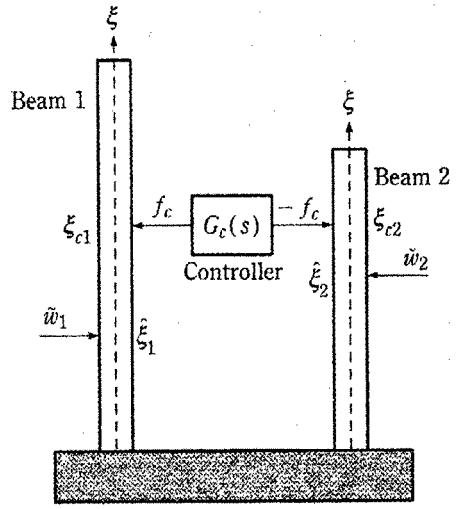

Fig. 12. Two cantilever beams with controller coupling.

$$\omega_{ij} = k_{ij}^2 \sqrt{\frac{E_i I_{Ai}}{m_i}},$$

$$\psi_{ij}(\xi_i) = A_{ij}[(\sin k_{ij} L_i - \sinh k_{ij} L_i)(\sin k_{ij}\xi - \sinh k_{ij}\xi) + (\cos k_{ij} L_i - \cosh k_{ij} L_i)(\cos k_{ij}\xi - \cosh k_{ij}\xi)],$$

where A_{ij} is the normalized parameter so that (5) holds and the wave number

k_{ij} satisfies

$$\cos k_{ij} L_i \cosh k_{ij} L_i = -1 .$$

Thus, a_{ij} and b_{ij} in (6) are given by $a_{ij} = \psi_{ij}(\hat{\xi}_i)$ and $b_{ij} = \psi_{ij}(\xi_{ci})$.

Now, we consider the first three modes of each beam and let $L_1 = 3$, $L_2 = 2.5$, $\rho_1 = \rho_2 = 1$, $E_1 I_{A1} = 1$, $E_2 I_{A2} = 1.1^2$, $\zeta_{1j} = 0.01$, $\zeta_{2j} = 0.02$, $j = 1, 2, 3$, $\hat{\xi}_1 = 1$, $\hat{\xi}_2 = 1.5$ and $\xi_{c1} = \xi_{c2} = 2.2$.

To reduce the vibration of the ith beam, $i = 1, 2$, we design four controllers. Controllers 1 and 2 are designed by the modal subsystem model to minimize $-\mathscr{P}_1^d$ and $-\mathscr{P}_2^d$, respectively, while Controllers 3 and 4 are designed by the structural subsystem model to minimize $-P_1^d$ and $-P_2^d$, respectively. The resulting energy flow diagrams are illustrated in Fig. 13 and 14 for the modal subsystem model and the structural subsystem model, respectively, where OL denotes the open-loop system and G_{ci} represents Controller i. Figures 13 and 14

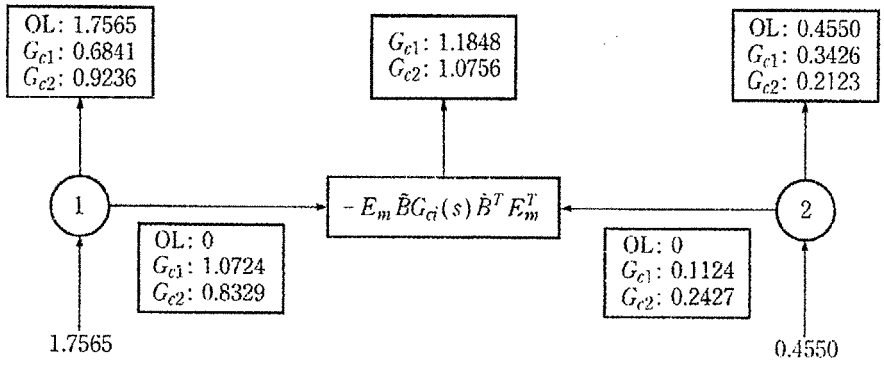

Fig. 13. Energy flow between beams with controllers G_{c1} and G_{c2} based on the modal subsystem model.

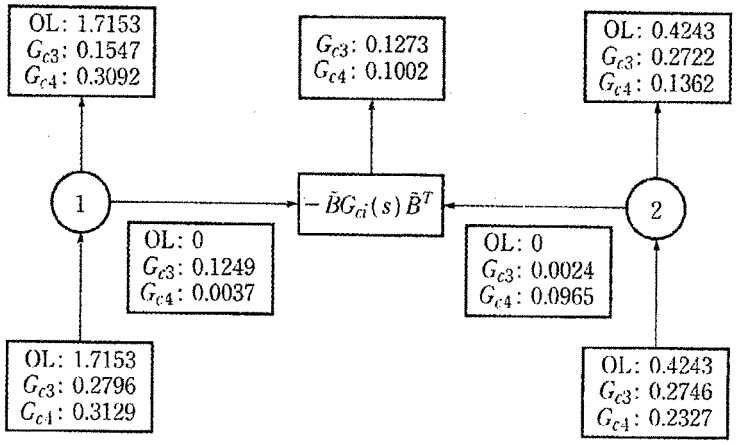

Fig. 14. Energy flow between beams with controllers G_{c3} and G_{c4} based on the structural subsystem model.

show that the controller absorbs energy from all of the subsystems and minimizes the energy dissipation from each beam. Furthermore, as explained in Example 1, Controllers 1 and 2 remove maximal energy from beams 1 and 2, respectively, while Controllers 3 and 4 minimize the total energy flow entering beams 1 and 2, respectively. The steady-state modal energy $\mathscr{E}_i$, $i = 1, 2$ is listed in Table 2, which shows that controllers designed by both models successfully reduce the modal energy of the specified beam. Furthermore, Fig. 15 shows that Controllers 1 and 2 are strictly positive real. Similar remarks apply to Controllers 3 and 4.

In this section, we obtained energy flow controllers based on both the modal subsystem model and the structural subsystem model. It is interesting to compare these two energy flow controllers. Since the structural energy flow model predicts energy flow among substructures, it is reasonable to expect that the controller based on this energy flow model is more effective than the controller based on the modal subsystem model. This fact is confirmed by Tables 1 and 2. In the structural subsystem model, however, the dynamics of the dissipation filter and the disturbance filter must be included in the augmented system, which increases the dimension of the controllers. For Example 1, the dimension of the controller for the modal subsystem model is 19, whereas for the structural subsystem model the controller order is 43.

Table 2. Steady-state modal energy for two coupled beams with relative force actuator

Modal energy	Open-loop	Controller 1	Controller 2	Controller 3	Controller 4
$\mathscr{E}_1$	2.3196	0.8441 (36.39[%])	1.7557 (75.69[%])	0.7882 (33.98[%])	1.6302 (70.28[%])
$\mathscr{E}_2$	0.6608	0.5434 (82.24[%])	0.2468 (37.35[%])	0.5051 (76.44[%])	0.2008 (30.93[%])

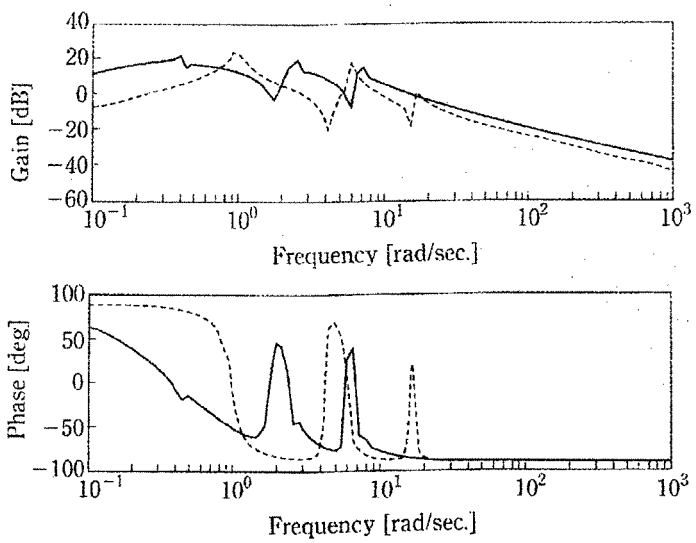

Fig. 15. Magnitude and phase of controllers G_{c1} (solid) and G_{c2} (dashed).

10. Conclusion

In this paper, we applied the control techniques developed for modal subsystems in Kishimoto et al. (1995 b) to structural subsystems, that is, interconnected structures. Based on these two energy flow models, strictly positive real controllers were designed as an additional subsystem or as a dissipative coupling by the LQG positive real control approach. The resulting controllers successfully minimizes the energy flow entering specified subsystems in H_2 sense and reduce the stored vibrational energy of the specified structure. These features were demonstrated by numerical examples.

References

Crandall, S.H. and R. Lotz (1971). On the coupling loss factor in statistical energy analysis. *J. Acoust. Soc. Amer.*, **49**, 352–356.

Davies, H.G. (1972). Power flow between two coupled beams. *J. Acoust. Soc. Amer.*, **51**, 393–401.

Kishimoto, Y. and D.S. Bernstein (1995 a). Thermodynamic modeling of interconnected systems: I. Conservative coupling. *J. Sound Vib.*, **182**, 23–58.

Kishimoto, Y. and D.S. Bernstein (1995 b). Thermodynamic modeling of interconnected systems: II. Dissipative coupling. *J. Sound Vib.*, **182**, 59–76.

Kishimoto, Y., D.S. Bernstein and S.R. Hall (1993). Dissipative control of energy flow in interconnected systems. *Proc. AIAA GNC Conference*, Monterey, CA, 657–666.

Kishimoto, Y., D.S. Bernstein and S.R. Hall (1995 a). Energy flow modeling of interconnected systems: A deterministic foundation for statistical energy analysis. *J. Sound Vib.*, **186** (to appear).

Kishimoto, Y., D.S. Bernstein and S.R. Hall (1995 b). Energy flow control of interconnected structures: I. Modal subsystem. *Control–Theory and Advanced Technology (C-TAT)*, **10**, 4, Part 4, 1563–1590.

MacMartin, D.G. and S.R. Hall (1991). Control of uncertain structures using an H_∞ power flow approach. *J. Guidance Control Dynamics*, **14**, 521–530.

Miller, D.W., S.R. Hall and A.H. Von Flotow (1990). Optimal control of power flow at structural junctions. *J. Sound Vib.*, **140**, 3, 475–497.

Norton, M.P. (1989). *Foundations of Noise and Vibration Analysis for Engineers*. Cambridge University Press, Cambridge.

Skudrzyk, E. (1968). *Simple and Complex Vibratory Systems*. Pennsylvania State University Press, PA.

Yasuo Kishimoto: see p.1590 in this issue.

Dennis S. Bernstein: see p.1590 in this issue.

Steven R. Hall: see p.1590 in this issue.